



**HAL**  
open science

## Differential predictive value of resident memory CD8+T cell subpopulations in patients with non-small-cell lung cancer treated by immunotherapy

Léa Paolini, Thi Tran, Stéphanie Corgnac, Jean-Philippe Villemin, Marie Wislez, Jennifer Arrondeau, Ludger Johannes, Jonathan Ulmer, Louis-Victorien Vieillard, Joséphine Pineau, et al.

### ► To cite this version:

Léa Paolini, Thi Tran, Stéphanie Corgnac, Jean-Philippe Villemin, Marie Wislez, et al.. Differential predictive value of resident memory CD8+T cell subpopulations in patients with non-small-cell lung cancer treated by immunotherapy. *Journal for Immunotherapy of Cancer*, 2024, 12 (12), pp.e009440. 10.1136/jitc-2024-009440 . hal-04955623

**HAL Id: hal-04955623**

**<https://hal.science/hal-04955623v1>**

Submitted on 19 Feb 2025






**HAL** is a multi-disciplinary open access archive for the deposit and dissemination of scientific research documents, whether they are published or not. The documents may come from teaching and research institutions in France or abroad, or from public or private research centers.

L'archive ouverte pluridisciplinaire **HAL**, est destinée au dépôt et à la diffusion de documents scientifiques de niveau recherche, publiés ou non, émanant des établissements d'enseignement et de recherche français ou étrangers, des laboratoires publics ou privés.



Distributed under a Creative Commons Attribution - NonCommercial 4.0 International License

# Differential predictive value of resident memory CD8<sup>+</sup>T cell subpopulations in patients with non-small-cell lung cancer treated by immunotherapy

Léa Paolini,<sup>1</sup> Thi Tran,<sup>1</sup> Stéphanie Corgnac,<sup>2</sup> Jean-Philippe Villemin,<sup>3</sup> Marie Wislez ,<sup>4,5</sup> Jennifer Arrondeau,<sup>6</sup> Ludger Johannes,<sup>7</sup> Jonathan Ulmer,<sup>7</sup> Louis-Victorien Vieillard,<sup>1</sup> Joséphine Pineau,<sup>1,8</sup> Alain Gey,<sup>1,8</sup> Valentin Quiniou,<sup>9</sup> Pierre Barennes,<sup>9</sup> Hang Phuong Pham,<sup>9</sup> Nadège Gruel ,<sup>10,11</sup> Milena Hasan,<sup>12</sup> Valentina Libri,<sup>12</sup> Sebastien Mella,<sup>12</sup> Sixtine De Percin,<sup>6</sup> Pascaline Boudou-Rouquette,<sup>6</sup> Aziza Caidi,<sup>2</sup> Isabelle Cremer ,<sup>5</sup> Hélène Blons,<sup>5,13</sup> Karen Leroy ,<sup>5,13</sup> Pierre Laurent-Puig,<sup>5,13,14</sup> Hortense De Saint Basile,<sup>1</sup> Laure Gibault,<sup>15</sup> Patrice Ravel,<sup>3</sup> Fathia Mami-Chouaib,<sup>2</sup> François Goldwasser,<sup>6</sup> Elizabeth Fabre,<sup>1,16</sup> Diane Damotte,<sup>5,17,18</sup> Eric Tartour <sup>1,8</sup>

**To cite:** Paolini L, Tran T, Corgnac S, *et al.* Differential predictive value of resident memory CD8<sup>+</sup>T cell subpopulations in patients with non-small-cell lung cancer treated by immunotherapy. *Journal for ImmunoTherapy of Cancer* 2024;**12**:e009440. doi:10.1136/jitc-2024-009440

► Additional supplemental material is published online only. To view, please visit the journal online (<https://doi.org/10.1136/jitc-2024-009440>).

LP, TT and SC are joint first authors.

Accepted 20 September 2024



© Author(s) (or their employer(s)) 2024. Re-use permitted under CC BY-NC. No commercial re-use. See rights and permissions. Published by BMJ.

For numbered affiliations see end of article.

**Correspondence to**  
Professor Eric Tartour;  
eric.tartour@aphp.fr

## ABSTRACT

**Background** A high density of resident memory T cells ( $T_{RM}$ ) in tumors correlates with improved clinical outcomes in immunotherapy-treated patients. In most clinical studies,  $T_{RM}$  are defined by the CD103 marker. However, it is clearly established that not all  $T_{RM}$  express CD103, but can be defined by other markers (CD49a, CD69, etc). The frequency of these subpopulations of  $T_{RM}$  expressing or not CD103 varies according to the location of the cancer. Little is known about their functionality and their predictive impact on response to immunotherapy. In preclinical models, only some subpopulations of  $T_{RM}$  are associated with cancer vaccine efficacy.

**Methods** Multiparametric cytometry analyses were used to demonstrate the presence of  $T_{RM}$  subpopulations in the lung in mice after vaccination and in fresh ex vivo human non-small cell lung cancer (NSCLC). An analysis of the T-cell repertoire of these  $T_{RM}$  was conducted to search for their relationships. Multiplex immunofluorescence techniques were used to quantify intratumor infiltration of  $T_{RM}$  subpopulations in two cohorts of patients with NSCLC. The impact on the clinical outcome of the  $T_{RM}$  tumor infiltration was also investigated.

**Results** We identified two main  $T_{RM}$  subpopulations in tumor-infiltrating lymphocytes derived from patients with NSCLC: one co-expressing CD103 and CD49a (double positive (DP)), and the other expressing only CD49a (simple positive (SP)); both exhibiting additional  $T_{RM}$  surface markers like CD69. Despite higher expression of inhibitory receptors, DP  $T_{RM}$  exhibited greater functionality compared with SP  $T_{RM}$ . Analysis of T-cell receptor (TCR) repertoire and expression of the stemness marker TCF1 revealed shared TCRs between populations, with the SP subset appearing more progenitor-like phenotype. In the training cohort, PD-L1 (Programmed Death-Ligand 1) and TCF1<sup>+</sup>CD8<sup>+</sup>T cells predict response to anti-PD-1. In patient with NSCLC validation cohorts, only DP  $T_{RM}$  predicted PD-1 blockade response. Multivariate analysis, including various

## WHAT IS ALREADY KNOWN ON THIS TOPIC

⇒ A population of resident memory CD8<sup>+</sup>T lymphocytes ( $T_{RM}$ ), initially identified by the marker CD103 and present in the tumor microenvironment, may be the target of anti-PD-1. Tumor infiltration by this CD103<sup>+</sup>CD8<sup>+</sup>T cell population is associated with a good prognosis. More recently, other  $T_{RM}$  subpopulations, expressing or not CD103, have been defined by other markers (CD49a, CD69, CXCR6) whose relationship, function and prognostic impact in the case of intratumoral infiltration are poorly understood.

biomarkers associated with responses to anti-PD-(L)1, such as total CD8, TCF1<sup>+</sup>CD8<sup>+</sup>T cells, and PD-L1, showed that only intratumoral infiltration by DP  $T_{RM}$  remained significant.

**Conclusions** This study highlights the non-equivalence of  $T_{RM}$  subpopulations. The population of  $T_{RM}$  co-expressing CD103 and CD49a appears to be the most functional and has the most significant capacity for predicting response to immunotherapy in multivariate analysis in patients with NSCLC.

## INTRODUCTION

More than two decades ago, pioneering work on vesicular stomatitis virus and *Listeria monocytogenes* revealed the presence and persistence of non-circulating resident memory T cells ( $T_{RM}$ ) in non-lymphoid organs after the resolution of the primary infection.<sup>1</sup> It rapidly became apparent that these  $T_{RM}$  constituted a specific lineage associated with a profile of transcription factors

### WHAT THIS STUDY ADDS

⇒ This study shows that there are two main populations of  $T_{RM}$  in non-small cell lung cancer (NSCLC), one co-expressing CD103 and CD49a and the other expressing CD49a only. They share many T-cell receptors, suggesting a common origin. Only intratumoral infiltration by  $T_{RM}$  co-expressing CD103 and CD49a can predict treatment response and survival in patients with NSCLC treated with an anti-PD-1 agent in first or second line therapy. In a multivariate analysis including infiltration by total  $CD8^+$ T cells,  $TCF1^+CD8^+$ T cells and the PD-L1 marker, the contribution of this subpopulation of resident T cells remained statistically significant.

### HOW THIS STUDY MIGHT IMPACT RESEARCH, PRACTICE OR POLICY

⇒  $T_{RM}$  are targets for anti-PD-1 therapy and are involved in the mechanism of action of cancer vaccines. This work shows that not all  $T_{RM}$  populations are equivalent and need to be better characterized for these purposes. Only one  $T_{RM}$  subpopulation is able to predict response to anti-PD-1 immunotherapy in patients with NSCLC. Its predictive impact is statistically robust after multivariate analysis including the reference marker PD-L1, which is already used in clinical practice in the choice of first-line treatment of these patients. The inclusion of this  $T_{RM}$  subpopulation in the initial work-up of these patients could improve their stratification and better personalize the different therapeutic options.

including Blimp1, Runx3, and Notch family proteins.<sup>2</sup> In terms of their phenotype, these  $T_{RM}$  express core markers such as CD69, CD103, and CD49a, together with the loss of expression of other markers such as CD62L, CCR7, S1PR1, and KLF2, favoring the persistence of these cells within tissues.<sup>3-4</sup>  $T_{RM}$  have innate-like “sensing and alarming” properties that enable them to recruit other immune cells to control microbial infections.<sup>5-7</sup> As they are located at the site of inflammation in the tissues,  $T_{RM}$  respond much more rapidly to reinfection and provide superior protection compared with circulating memory cells, including central memory and effector memory T cells.<sup>5,6,8</sup>

In a range of preclinical cancer models, we have shown that  $T_{RM}$  are required for the efficacy of antitumor vaccines against mucosal tumors such as lung and head and neck cancer.<sup>9,10</sup> In humans, high levels of intratumoral  $T_{RM}$  infiltration have been associated with better clinical outcomes in multiple solid tumors including lung, melanoma, bladder, breast, cervical, ovarian, endometrial, gastric, and colorectal cancers receiving standard-of-care treatments.<sup>10-12</sup> More recently in humans, correlative studies in non-small cell lung cancer (NSCLC), bladder cancer, and melanoma have revealed an association between tumor infiltration by  $CD8^+$  T cells with a resident phenotype before immunotherapy and responses to immune checkpoint blockade.<sup>13-16</sup>

To explain this predictive role of  $T_{RM}$  during immunotherapy, various groups have shown that during neoadjuvant treatment in breast and head and neck cancers,  $CD8^+$  tumor-infiltrating lymphocytes (TILs) with a tissue-resident phenotype expand and are characterized by a

gene expression program related to activation, cytotoxicity, and effector functionality.<sup>17</sup> The same expansion of  $CD8^+$   $T_{RM}$  has been observed after anti-PD-1/PD-L1 monotherapy or combined anti-CTLA-4 treatment in melanoma, lung, breast, and esophageal cancers.<sup>13,18,19</sup> The role of  $T_{RM}$  as immunotherapeutic targets raises the possibility that other effectors recruited secondarily or present in the blood may play a role in the efficacy of immunotherapy.<sup>20</sup>

Given the antitumor role of  $T_{RM}$  and their prognostic and predictive value in the context of patient responses to immunotherapy, the issue of optimal strategies for inducing or increasing this population is becoming a major challenge in immuno-oncology. In preclinical models, we have shown that the nasal route, but not the muscular route, induces  $T_{RM}$  with a  $CD103^+CD49a^+CD69^+$  phenotype.<sup>9,10</sup> This induction was associated with the inhibition of the growth of lung or head and neck tumors. In infectious and oncological models, other groups have also documented a correlation between the preferential ability of mucosal immunization to induce  $T_{RM}$  expansion and protection against the development of cancers and viral infections.<sup>21</sup> However, other studies based on vaccinations using systemically administered recombinant viral vectors have shown that  $T_{RM}$  can be induced in the lungs.<sup>22</sup> This result may be explained by the use of viruses that enable vaccine dissemination in the pulmonary or head and neck compartments. However, messenger RNA-based vaccinations have also been shown to induce  $T_{RM}$  when administered via the intramuscular (i.m.) route, but the cells induced in this context generally express CD69 or CD49a without any concomitant CD103 expression.<sup>23</sup> The fact that different subpopulations of  $T_{RM}$  exist with differing core marker (CD103, CD49a, CD69) expression patterns has been reported in various tissues, and this effect has sometimes been linked to the different functions of these cells.<sup>24</sup> Although CD103 is considered a hallmark of  $T_{RM}^P$ , persistent CD103-negative ( $CD103^{neg}$ )  $T_{RM}$  have also been described in tissues. In contrast with  $CD103^+$   $T_{RM}^P$ , these cells were able to develop in a transforming growth factor beta (TGF- $\beta$ )-independent manner.<sup>25</sup>

In this work, we aimed to better characterize these different  $T_{RM}$  subpopulations in mice and humans and to determine whether they play distinct roles as predictors of responses to immunotherapy in patients with NSCLC.

## RESULTS

### Different immunization routes give rise to distinct subpopulations of resident memory $CD8^+$ T lymphocytes

Our previous work had shown that only the intranasal (i.n) immunization route induced resident memory  $CD103$ -expressing  $CD8^+$ T cells in bronchoalveolar lavage fluid (BAL), and this mucosal immunization route was associated with tumor rejection.<sup>10</sup> In recent years, it has emerged that there are different  $T_{RM}$  subpopulations defined by the markers CD103, CD49a, and CD69.<sup>4</sup> In the present study, only i.n vaccination with the STxB-E7 vaccine combined

with alpha-galactosylceramide ( $\alpha$ GalCer)-induced D<sup>b</sup>-restricted E7<sub>49–57</sub> peptide-specific CD8<sup>+</sup>T cells co-expressing CD103 and CD49a in the BAL (figure 1A). In contrast, the i.m. route also induced E7-specific CD8<sup>+</sup> T cells expressing CD49a but not CD103 (figure 1A). Both CD103<sup>+</sup>CD49a<sup>+</sup> and CD103<sup>neg</sup>CD49a<sup>+</sup>CD8<sup>+</sup> T-cell populations induced by the i.n route expressed high levels of CD69 (for CD103<sup>+</sup>CD49a<sup>+</sup>: mean 94.82%±1.86% and for CD103<sup>neg</sup>CD49a<sup>+</sup> mean: 95.5%±1.49%) (figure 1A, lower right), whereas the frequency of CD8<sup>+</sup> T cells specific for E7 and expressing neither CD103 nor CD49a, which are considered to be effector T cells, exhibited weaker CD69 expression (mean 49.24%±10.24%) (figure 1A, lower right). Immunization via the i.n route induced a marginal CD103<sup>+</sup>CD49a<sup>-</sup> T-cell population (<5%) (figure 1).

It should be noted that i.m.-induced CD49a<sup>+</sup>CD103<sup>+</sup>CD8<sup>+</sup>T cells were less likely to express CD69 as compared with i.n-induced ones (mean: 68.4%±11.6%) (figure 1A, upper right), but their numbers were equivalent in the BAL irrespective of the immunization route (figure 1B). These results were replicated by analyzing the same resident memory CD8<sup>+</sup> T-cell subpopulations in lung parenchyma after i.m. or i.n vaccination (online supplemental figure S2A,B).

Similarly, using another vaccine system consisting of the protein ovalbumin mixed with the adjuvant c-di-GMP, only immunization via the i.n route induced ovalbumin-specific CD103-expressing CD8<sup>+</sup>T cells in the BAL (online supplemental figure 2C,D). The subcutaneous route, like the i.m. route above, induced only CD103<sup>neg</sup>CD49a<sup>+</sup>CD8<sup>+</sup>T cells (online supplemental figure S2C,D). Single-cell transcriptomic analyses in lung tumor-bearing mice showed that the CD49a<sup>+</sup>CD103<sup>neg</sup> T-cell population expressed CD69 as well as other resident markers (Zfp683, Runx3, Blimp1, Fabp5), but no lymph node homing markers such as Sell (online supplemental figure S4A). Characterization of these resident memory E7-specific CD8<sup>+</sup> T-cell subpopulations (CD103<sup>+</sup>CD49a<sup>+</sup> and CD103<sup>neg</sup>CD49a<sup>+</sup>) revealed that the CD103<sup>+</sup>CD49a<sup>+</sup>CD8<sup>+</sup>T cells expressed more PD-1 (mean: 78.04%±9.65%) as compared with the CD103<sup>neg</sup>CD49a<sup>+</sup> population (mean 62.66%±8.14%) and the CD103<sup>neg</sup>CD49a<sup>neg</sup> effector CD8<sup>+</sup> T-cell population (mean: 47.46%±7.03%) (figure 1C). Interestingly, the resident memory CD8<sup>+</sup> T-cell population co-expressing CD103 and CD49a appeared to be more functional after antigenic stimulation with a peptide derived from the E7 protein, secreting more interferon (IFN)- $\gamma$ , tumor necrosis  $\alpha$  (TNF- $\alpha$ ), CCL4, and CCL5 (figure 1D) highlighting the more functional and protective phenotype of these cells.

### Distinct subpopulations of T<sub>RM</sub>-type CD8<sup>+</sup>T lymphocytes coexist among lung TILs

To determine whether the same T<sub>RM</sub> populations are present in human lung tumors and to compare their phenotype, TILs were obtained from 20 dissociated tumors from patients with NSCLC. The same T<sub>RM</sub> subpopulations identified in mice (CD103<sup>+</sup>CD49a<sup>+</sup>

and CD103<sup>-</sup>CD49a<sup>+</sup>) were detected in humans, with the CD103<sup>+</sup>CD49a<sup>+</sup> population being present at a higher frequency (mean: 47%±22.52% of total CD8) (figure 2A). Nearly all of these T<sub>RM</sub> exhibited an effector memory T-cell phenotype (CCR7<sup>-</sup>CD45RA<sup>-</sup>) (online supplemental figure S3). The two T<sub>RM</sub> subpopulations expressed CD69 at a higher frequency (mean %CD69<sup>+</sup>: 87.2%±6.9% in CD103<sup>+</sup>CD49a<sup>+</sup> and 66.6%±12.8% in CD103<sup>neg</sup>CD49a<sup>+</sup>) as compared with the effector CD8<sup>+</sup>T cell population (CD103<sup>neg</sup>CD49a<sup>neg</sup>; 33.8%±14.12%) (figure 2B). The CD103<sup>+</sup>CD49a<sup>+</sup> cells expressed exhaustion markers (PD-1, T-cell immunoglobulin mucin 3 (Tim-3), CD39) and the proliferation marker Ki67 significantly more frequently (figure 2B). These data were confirmed by single-cell transcriptomic analyses of intratumoral CD8<sup>+</sup>T cells, which showed that the resident memory CD103<sup>+</sup>CD49a<sup>+</sup>CD8<sup>+</sup> T cells exhibited higher expression levels of exhaustion, cytotoxicity and proliferation markers compared with the CD103<sup>neg</sup>CD49a<sup>+</sup>CD8<sup>+</sup>T cell population (online supplemental figure S4B). Based on our own cohort data set and the re-analyzed data set from Clarke *et al.*,<sup>26</sup> we also showed that the CD103<sup>+</sup>CD49a<sup>+</sup>CD8<sup>+</sup> T cells expressed higher levels of cytokines (IFN- $\gamma$ , interleukin (IL)-2) and chemokines (CCL3, CXCL13) (online supplemental figure S4B,C).

We regard the CD103<sup>neg</sup>CD49a<sup>+</sup> population as a T<sub>RM</sub> population, as most of these cells express CD69, which is considered to be a T<sub>RM</sub> marker.<sup>3</sup> Interestingly, as opposed to the non-resident CD103<sup>neg</sup>CD49a<sup>neg</sup> CD8<sup>+</sup> T cells, they do not express the circulating and lymph node homing markers (SELL, S1PR1) or the KLF2 transcription factor (online supplemental figure S4D).

In contrast, they express the transcription factors Hobit (ZNF683) and Runx3, which are hallmarks of T<sub>RM</sub>. However, unlike to mouse T<sub>RM</sub>, these transcription factors are not enriched in human T<sub>RM</sub> (online supplemental figures S4D and S5).<sup>2</sup>

### Relationship between the T<sub>RM</sub> subpopulations in terms of differentiation

To define the relationship or not between these two main T<sub>RM</sub> populations, a comparative analysis of the T-cell receptor (TCR) repertoire of these cells and differentiation markers was carried out.

Four fresh tumors were used to conduct single-cell transcriptomic analyses, revealing that, among all the patients, the five most frequent clonotypes (TRA or TRB) of the double positive T<sub>RM</sub> CD8<sup>+</sup>T cell subpopulation (CD103<sup>+</sup>CD49a<sup>+</sup>) were also present in the single positive T<sub>RM</sub> CD8<sup>+</sup> T-cell subpopulation (CD103<sup>neg</sup>CD49a<sup>+</sup>) as well as in the CD103<sup>neg</sup>CD49a<sup>neg</sup> effector CD8<sup>+</sup> T-cell population (figure 3A). These clonotypes were most amplified in the CD103<sup>+</sup>CD49a<sup>+</sup>CD8<sup>+</sup> T cells, followed by the CD103<sup>neg</sup>CD49a<sup>+</sup>CD8<sup>+</sup>T cell population and finally the CD103<sup>neg</sup>CD49a<sup>neg</sup> CD8<sup>+</sup>T cell population (figure 3B), suggesting possible differentiation and

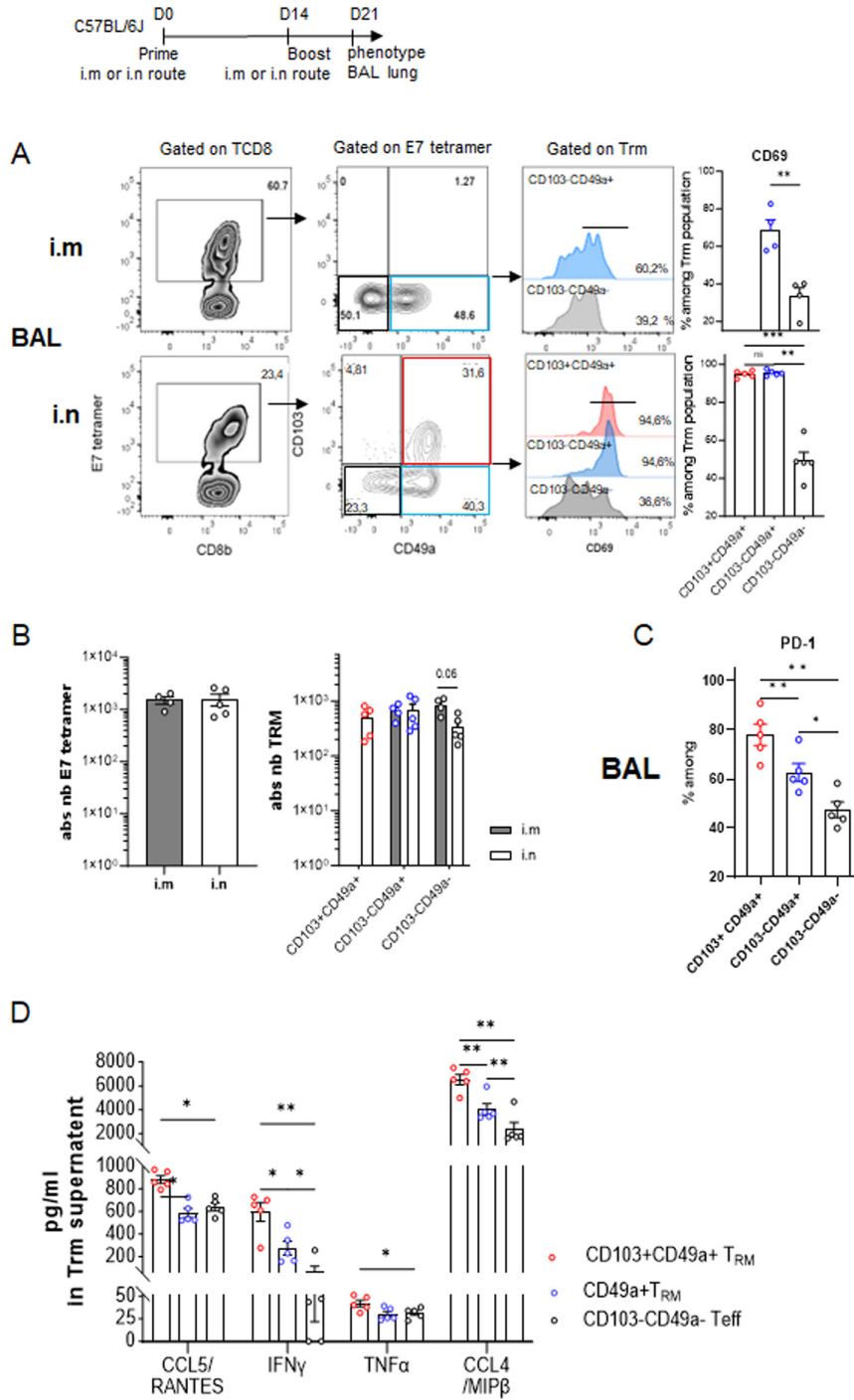


**Figure 1** Various subpopulation of specific T<sub>RM</sub> with different phenotypes and functionality are induced depending on the route of immunization. C57BL/6J mice were immunized with STxB-E7 and alpha-galactosylceramide by intranasal (i.n) or intramuscular (i.m.) route at day 0 and 14, then sacrificed at day 21, CD8a APCeFluo 780 (5  $\mu$ g) were injected intravenous 5 min before sacrifice to discriminate circulating CD8<sup>+</sup>T cells and resident CD8<sup>+</sup>T cells. (A) Representative flow cytometry plots in BAL (broncho-alveolar lavage) of specific E7-tetramer, CD103<sup>+</sup>CD49a<sup>+</sup> T<sub>RM</sub>, CD103<sup>-</sup>CD49a<sup>+</sup> T<sub>RM</sub> and CD103<sup>-</sup>CD49a<sup>-</sup> Teff, and CD69 frequency among these populations. (B) Absolute number of (left) E7-tetramer CD8<sup>+</sup> and (right) CD103<sup>+</sup>CD49a<sup>+</sup> T<sub>RM</sub>, CD103<sup>-</sup>CD49a<sup>+</sup> T<sub>RM</sub> and Teff CD103<sup>-</sup>CD49a<sup>-</sup> in BAL. Datas are expressed as mean $\pm$ SEM. One representative experiment with three to five mice from two independent experiments is shown. Analysis of difference within groups were performed with two-side Mann-Whitney t-test. (C) Percentage of PD-1 among E7-specific CD103<sup>+</sup>CD49a<sup>+</sup> T<sub>RM</sub>, CD103<sup>-</sup>CD49a<sup>+</sup> T<sub>RM</sub> and CD103<sup>-</sup>CD49a<sup>-</sup> Teff in the BAL. (D) E7-specific CD103<sup>+</sup>CD49a<sup>+</sup> T<sub>RM</sub>, CD103<sup>-</sup>CD49a<sup>+</sup> and CD103<sup>-</sup>CD49a<sup>-</sup> Teff were sorted from BAL at D21, and stimulated (10,000 cells/well) with E7<sub>49-57</sub> peptide (10  $\mu$ g/mL) for 18 hours. Then supernatant were harvested and cytokines multiplex assay was performed. Datas are expressed as mean $\pm$ SEM. One representative experiment with three to five mice from two independent experiments is shown. Analysis of difference within groups were performed with one-way analysis of variance paired-test with Tukey multiple comparison. \*p<0,05 \*\*p<0,01 \*\*\*p<0001 \*\*\*\*p<0,0001. IFN, interferon; PD-1: programmed cell death 1; TNF: tumor necrosis factor; T<sub>RM</sub>: resident memory T cells.

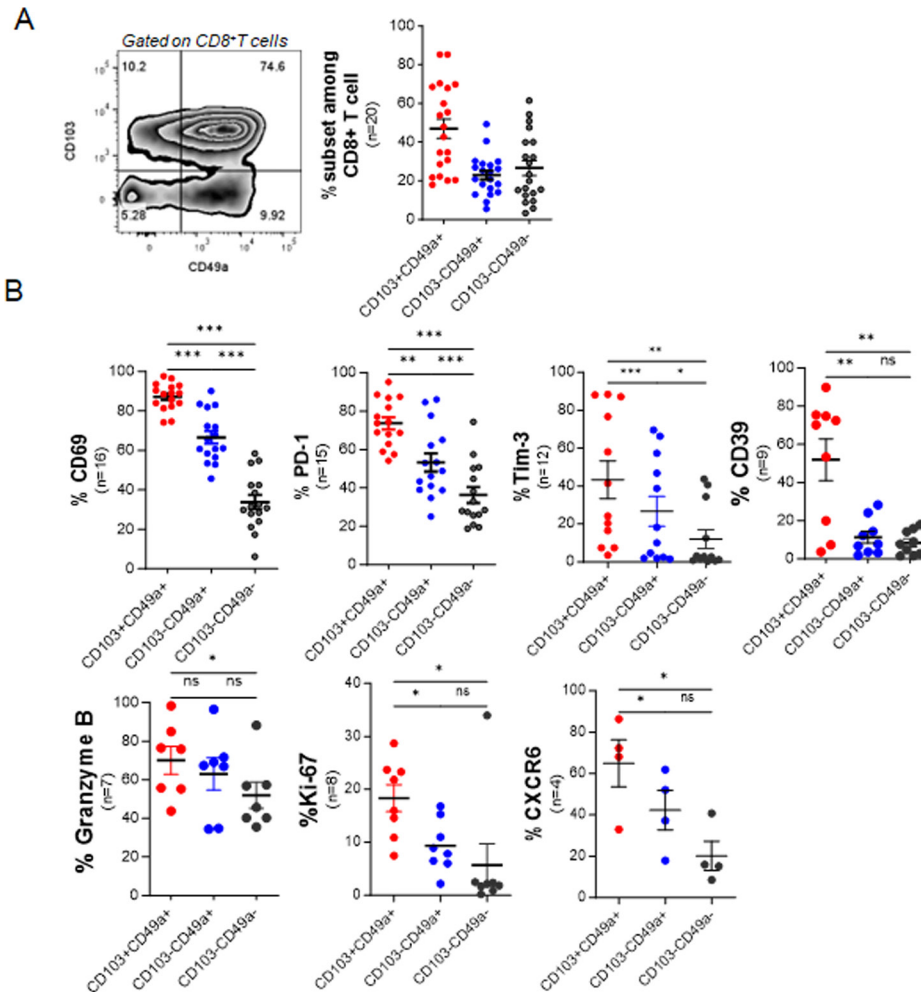


**Figure 2** Phenotypic analyses of subpopulations of  $T_{RM}$  and effector T cells among TILs derived from patients with lung cancer. Fresh biopsies from patients with lung cancer ( $n=20$ ) were dissociated and digested, and flow cytometry was used to analyze TILs. The number of TILs tested per marker is shown below each figure. (A) The percentages of  $T_{RM}$  subpopulations ( $CD103^+CD49a^+$  and  $CD49a^+CD103^-$ ) among  $CD8^+T$  cells, as well as non-effectors  $T_{RM}$  ( $CD49a^-CD103^-$ ) among  $CD8^+T$  cells are shown. (B) The percentages of different markers defining  $T_{RM}$  (CD69, CXCR6), exhausted T cells (PD-1, Tim-3, CD39), cytotoxicity (GZMB), and proliferation (Ki67) are shown among the two populations of  $T_{RM}$  and non- $T_{RM}$  effectors ( $CD103^-CD49a^-$ ). Significance was determined using paired t-tests.  $p<0.05$  was regarded as statistically significant. \* $p<0.05$ , \*\* $p<0.01$ , \*\*\* $p<0.001$ ;  $n=4-20$ . TIL, tumor-infiltrating lymphocyte; TIM-3: T-cell immunoglobulin mucin 3; GZMB: granzyme B; PD-1: programmed cell death 1; TRM, resident memory T cells.

proliferation of effector  $CD8^+$  T lymphocytes into the resident memory  $CD103^{neg}CD49a^+CD8^+$  T cells and then into resident memory  $CD103^+CD49a^+CD8^+$  T cells. Based on the Jaccard and the Morisita-horn dissimilarity indices (figure 3C,D, respectively), we found that for three out of four patients analyzed, closer repertoire composition and less dissimilarity (index close to 0) was observed between the  $CD103^+CD49a^+$  and the  $CD103^{neg}CD49a^+CD8^+$  T cell populations as compared with the  $CD103^{neg}CD49a^{neg}$  population, reinforcing the relationship between the two  $T_{RM}$  populations. With respect to the trajectories of these three subpopulations, another argument supports a more terminal differentiation of the  $CD103^+CD49a^+$   $T_{RM}$  population since they express less TCF1, a progenitor marker (online supplemental figure S6). Indeed, in mice, the % of cells

expressing TCF1, a stemness marker, is lower (mean  $57.03\% \pm SD 6.37\%$ ) in the  $CD103^+CD49a^+CD8^+$  T cell population, than in the  $CD103^{neg}CD49a^+CD8^+$  T cells (mean  $73.1\% \pm 5.45\%$ ) and in the  $CD103^{neg}CD49a^{neg}$  effector  $CD8^+$  T populations (mean  $71.78\% \pm 9.45\%$ ) (online supplemental figure S6). In humans, multiplex in situ immunofluorescence imaging revealed that the  $CD103^+CD49a^+CD8^+$  T cell population does not express TCF1 (results not shown), as described previously.<sup>27</sup>

To confirm this relationship and the possible difference in the stage of differentiation between these T-cell populations, we performed pseudotime trajectory inference analysis on the transcriptome single cell RNA-seq (scRNA-seq) data. We can observe a differentiation from the double negative (DN) population ( $CD103^{neg}CD49a^{neg}$ ) to the DP (double positive) population ( $CD103^+CD49a^+$ ) via the

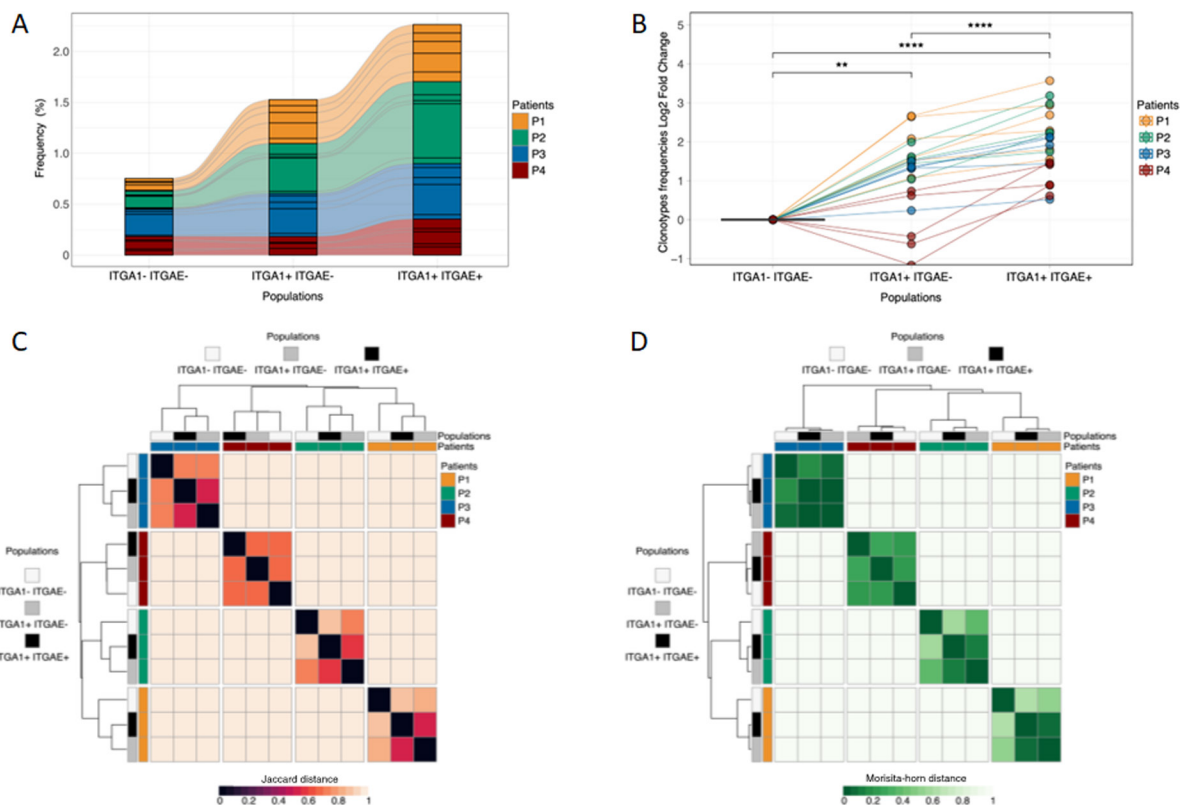


**Figure 3** T-cell receptor sharing among the subpopulations of resident memory CD8<sup>+</sup>T cells. (A) Tracking of the most predominant clonotypes within the ITGA1<sup>+</sup>(CD49a)/ITGAE<sup>+</sup> (CD103) population. Alluvial plots represent the relationships between the frequencies of the five most predominant T-cell clonotypes detected within the ITGA1<sup>+</sup>/ITGAE<sup>+</sup> population (right barplot), in the ITGA1<sup>neg</sup>/ITGAE<sup>neg</sup> (left barplot) and ITGA1<sup>+</sup>/ITGAE<sup>neg</sup> (middle barplot) populations for each patient. Each square represents the frequency of a clonotype in the corresponding population. (B) Fold change of the most predominant clonotypes within the ITGA1<sup>+</sup>/ITGAE<sup>+</sup> population. Dots represent the five most predominant T-cell clonotypes detected in the ITGA1<sup>+</sup>/ITGAE<sup>+</sup> population observed using the log<sub>2</sub> fold change in ITGA1<sup>+</sup>/ITGAE<sup>+</sup> (right) and ITGA1<sup>+</sup>/ITGAE<sup>neg</sup> (middle) compared with the ITGA1<sup>neg</sup>/ITGAE<sup>neg</sup> (left) cell populations by patient. Each dot is linked across cell populations by a line colored by patient. Statistical analysis was performed using paired Student's t-tests (\*\*\*\*p<0.0001, \*\*p<0.01). (C) Jaccard overlap among repertoires was analyzed by generating a heatmap of the Jaccard dissimilarity index calculated across the three cell populations: ITGA1<sup>neg</sup>/ITGAE<sup>neg</sup> (white), ITGA1<sup>+</sup>/ITGAE<sup>neg</sup> (gray), and ITGA1<sup>+</sup>/ITGAE<sup>+</sup> (black). The Euclidean distance was used for hierarchical clustering as a color-coded matrix ranging from 0 (minimum dissimilarity) to 1 (maximum dissimilarity). (D) Morisita horn overlap among repertoires was analyzed by generating a heatmap of the Morisita horn dissimilarity index calculated across the three cell populations: ITGA1<sup>neg</sup>/ITGAE<sup>neg</sup> (white), ITGA1<sup>+</sup>/ITGAE<sup>neg</sup> (gray), and ITGA1<sup>+</sup>/ITGAE<sup>+</sup> (black). The Euclidean distance was used for hierarchical clustering as a color-coded matrix ranging from 0 (minimum dissimilarity) to 1 (maximum dissimilarity). Patients included in this figure are color-coded as patient 1 (orange), patient 2 (green), patient 3 (blue), and patient 4 (red).

SP population (CD103<sup>neg</sup>CD49a<sup>+</sup>) (online supplemental figure S7).

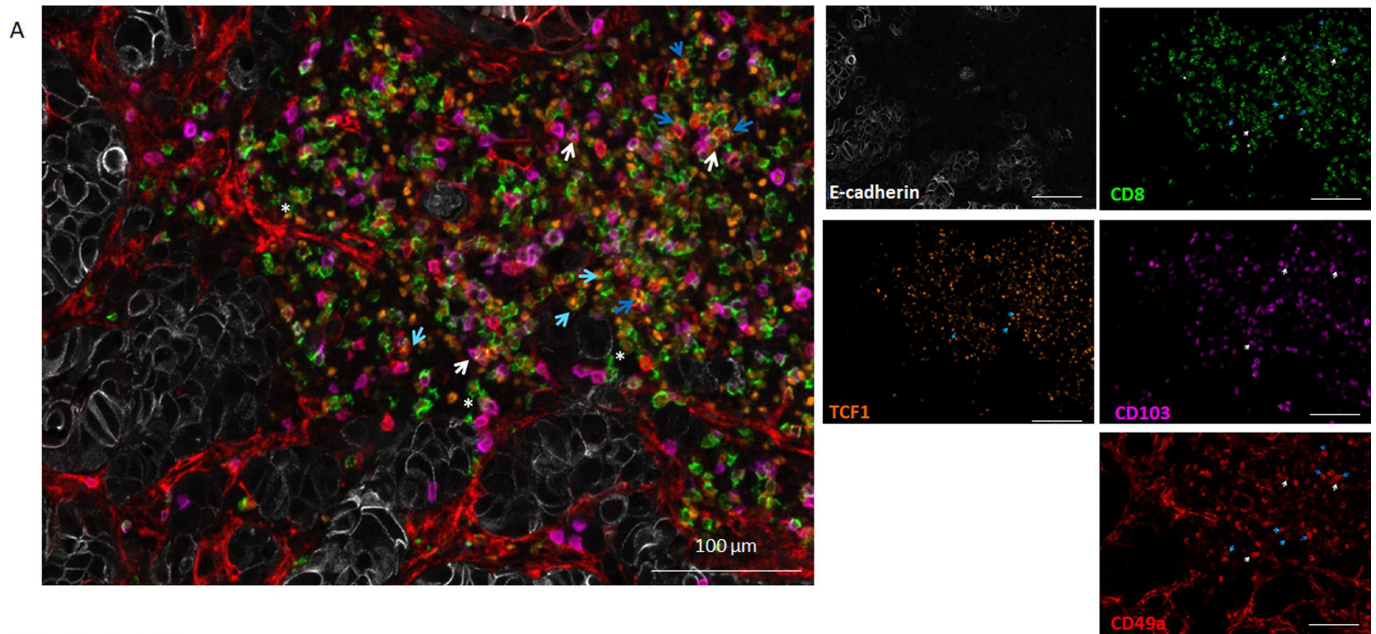
### Distribution and infiltration of lung tumors by resident memory CD8<sup>+</sup> T-cell subpopulations

The distribution and location of the different T<sub>RM</sub> subpopulations were then determined using a multiplex in situ immunofluorescence.

This technique has enabled us to compare infiltration by different T<sub>RM</sub> subpopulations either in the tumorous or stromal zone (figure 4A). We also included the TCF1 marker when conducting this staining (figure 4A), as it is often considered a marker of stemness potentially associated with response to immunotherapy.<sup>28</sup> We observed a higher density of total CD8<sup>+</sup>T cells, as well as all T<sub>RM</sub> subpopulations, in the stroma compared with the tumor zone (figure 4B). In the tumor, the CD103<sup>+</sup>CD49a<sup>+</sup> CD8<sup>+</sup>

T<sub>RM</sub> population was more frequently detected (mean: 20±62 cells/mm<sup>2</sup>) as compared with the CD103<sup>-</sup>CD49a<sup>+</sup>CD8<sup>+</sup> T<sub>RM</sub> population (mean: 9±11 cells/mm<sup>2</sup>), but with no statistical difference. Both populations were also present in the stroma at higher density (mean: 119±179 cells/mm<sup>2</sup> for CD103<sup>+</sup>CD49a<sup>+</sup> CD8<sup>+</sup> T cells; mean: 92±84 cells/mm<sup>2</sup> for CD103<sup>-</sup>CD49a<sup>+</sup>CD8<sup>+</sup>T cells) (figure 4B). The CD49a marker has also been reported to be expressed by endothelial cells<sup>29</sup> (figure 4A). Since E-cadherin interacts with the CD103 molecule, we investigated whether the CD103<sup>+</sup>CD8<sup>+</sup>T cell population interacted more with E-cadherin<sup>+</sup> cells than the CD103<sup>neg</sup>CD8<sup>+</sup>T cells.

We measured the % interaction between CD103<sup>+</sup>CD8<sup>+</sup>T cells or CD103<sup>neg</sup>CD8<sup>+</sup>T cells with E-cadherin using Akoya phenoptReport software. We considered an interaction between E-cadherin and CD8<sup>+</sup>T cells when the



White star\* CD8<sup>+</sup>Tcf1<sup>+</sup>  
 White arrow CD8<sup>+</sup>CD49a<sup>+</sup>CD103<sup>-</sup>Tcf1<sup>-</sup>  
 Blue arrow CD8<sup>+</sup>CD49<sup>-</sup>CD103<sup>-</sup>Tcf1<sup>-</sup>  
 Cyan arrow CD8<sup>+</sup>CD49<sup>-</sup>CD103<sup>-</sup>Tcf1<sup>+</sup>

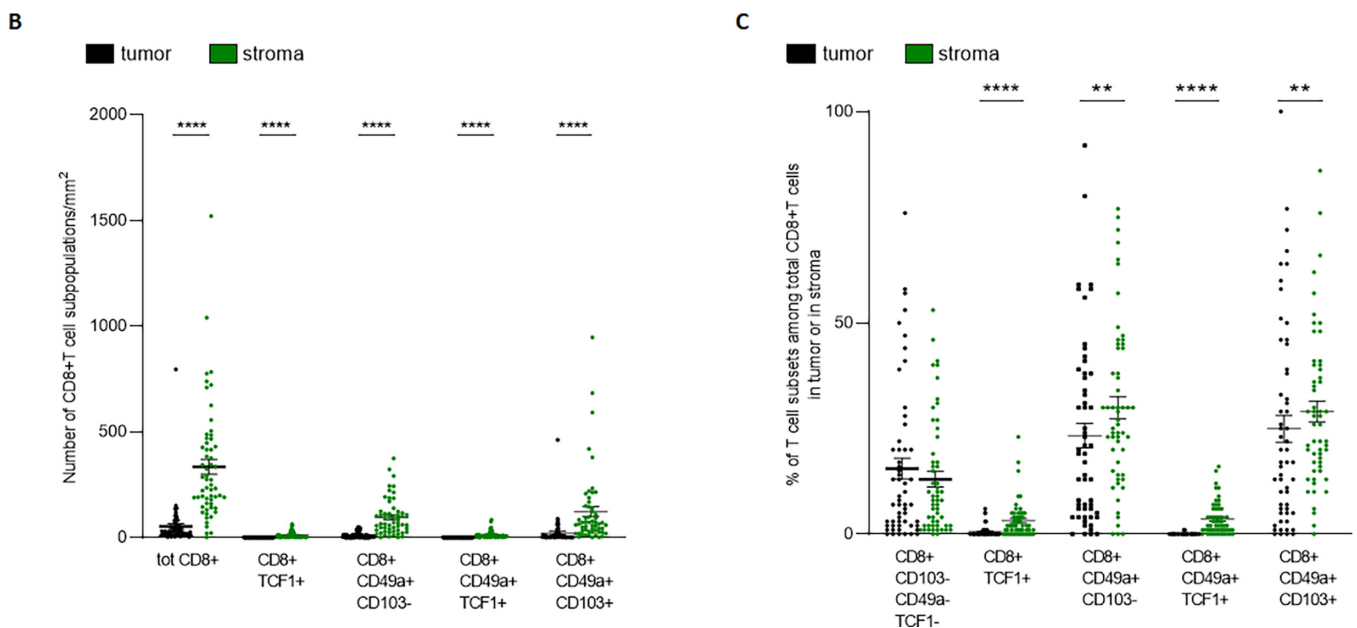


**Figure 4** Infiltration of non-small cell lung cancers by subpopulations of resident memory CD8<sup>+</sup> T lymphocytes. (A) Representative image of the infiltration of non-small cell lung cancer. Multiplexed immunostaining was performed on paraffin-embedded tissues with antibodies to detect CD8, CD103, TCF1, CD49a and E-cadherin. inForm software enabled cell phenotyping and tissue segmentation that was performed with E-cadherin staining to discriminate tumor and stromal areas. Automated counting and mapping enabled the phenotyping of T cells: subpopulations of non-T<sub>RM</sub> tumor-infiltrating lymphocyte (defined as CD8<sup>+</sup>CD49a<sup>-</sup>CD103<sup>-</sup>TCF1<sup>+</sup>) and of CD8<sup>+</sup> T<sub>RM</sub> lymphocytes defined as CD8<sup>+</sup>CD49a<sup>+</sup>CD103<sup>+</sup>TCF1<sup>-</sup> (white arrow), CD8<sup>+</sup>CD49a<sup>+</sup>CD103<sup>-</sup>TCF1<sup>+</sup>, CD8<sup>+</sup>CD49a<sup>+</sup>CD103<sup>-</sup>TCF1<sup>-</sup>. Original magnification  $\times 200$ . Cell number (B) and percentage (C) of non-T<sub>RM</sub> and CD8<sup>+</sup> T<sub>RM</sub> lymphocytes tumor-infiltrating lymphocytes were determined by in situ immunofluorescence. Each dot represents one patient. The average number of fields counted per patient is 16. Isotype control antibodies were done for each experiment. Significance was determined by a Wilcoxon test. Values of  $p < 0.05$  were considered statistically significant. \*\* $p < 0.01$ ; \*\*\*\* $p < 0.0001$ . T<sub>RM</sub>, resident memory T cells.

distance between these cells was  $< 15 \mu\text{m}$ . We observed that CD103<sup>+</sup>CD8<sup>+</sup>T cells interacted more strongly with E-cadherin than the CD103<sup>neg</sup>CD8<sup>+</sup>T cells (online supplemental figure S8).

The TCF1<sup>+</sup>CD8<sup>+</sup>T cell population also infiltrated the tumor microenvironment in these patients, but these cells were only found in the stroma (mean:  $11 \pm 15$  cells/mm<sup>2</sup>) and not in the tumor nest. CD103<sup>+</sup>CD49a<sup>+</sup>CD8<sup>+</sup>



T cells were not found to express TCF1, but 13% of the CD103<sup>+</sup>CD49a<sup>+</sup>CD8<sup>+</sup> T cells expressed TCF1 (figure 4B,C). TCF1 expression was mainly observed in the stromally localized populations but not in the epithelial tumor islets (figure 4B,C).

### The resident memory CD103<sup>+</sup>CD49a<sup>+</sup>CD8<sup>+</sup>T cell population is the strongest predictor of clinical responses to anti-PD-1 immunotherapy

The prognostic impact of these different T<sub>RM</sub> subpopulations was then evaluated, taking into account their location within the tumor microenvironment. We also analyzed the TCF1-expressing T-cell population, which is considered to be the target of anti-PD-1 therapy, and whose pretreatment infiltration is the best predictor of anti-PD-1 response.<sup>28 30–32</sup>

Cox proportional-hazards univariate analysis showed that PD-L1 remained the most predictive biomarker of clinical response (HR=3.06 (0.002–6.31), p=0.002) in patients with NSCLC undergoing second-line treatment with anti-PD-1 (figure 5A). Interestingly, the population of T<sub>RM</sub> CD8<sup>+</sup> T cells localized in the tumor co-expressing CD103 and CD49a markers was also a pretreatment feature correlated (HR=2.41 (1.26–4.62), p=0.008) with clinical response (figure 5A), but this association did not remain true in the stroma (HR=1.76 (0.092–3.39), p=0.09). Intratumoral infiltration by CD103<sup>+</sup>CD49a<sup>+</sup>CD8<sup>+</sup>T cells did not predict clinical response as defined by the response evaluation criteria in solid tumors (RECIST) criteria (data not shown).

In the same analysis, total CD8<sup>+</sup> T cells (HR=2.00 (1.04–3.84), p=0.037) and TCF1-expressing CD8<sup>+</sup> T cells (HR=2.11 (1.09–4.06), p=0.025) also served as biomarkers associated with clinical response (figure 5A). In contrast, the resident memory CD103<sup>+</sup>CD49a<sup>+</sup>CD8<sup>+</sup> T-cell population, did not predict clinical response to immunotherapy (figure 5A) irrespective of its stromal or tumorous location (HR=1.66 (0.87–3.17), p=0.12 and HR=1.70 (0.89–3.22), p=0.106, respectively).

These results were confirmed through Kaplan-Meier survival curve analyses and log-rank tests, confirming the relationships between survival and infiltration by CD103<sup>+</sup>CD49a<sup>+</sup> CD8<sup>+</sup>T cells, total CD8 and stromal TCF1<sup>+</sup>CD8<sup>+</sup>T cells, well as the expression of PD-L1 by tumor cells (TCs) (figure 5B). In contrast, only PD-L1 expression (>1%) by TCs and infiltration in the stroma by TCF1<sup>+</sup>CD8<sup>+</sup> T cells were correlated with progression-free survival (PFS) (HR=2.89 (1.52–5.5), p=0.01 and HR=1.84 (1.02–3.31), p=0.043) in these immunotherapy-treated patients (online supplemental figure S9A). This observation was made when comparing two groups of patients dichotomized using the median values for the parameters of interest. When we focused on extreme values using tertiles as cut-offs, the intratumoral CD103<sup>+</sup>CD49a<sup>+</sup> CD8<sup>+</sup> cell population appeared to be also prognostic variable for PFS (HR=2.22 (1.05–4.67), p=0.036) (online supplemental figure S9B).

Receiver operating characteristic (ROC) curve analyses of CD103<sup>+</sup>CD49a<sup>+</sup>CD8<sup>+</sup>T cell infiltration yielded an area under the curve (AUC) of 0.88 when predicting overall survival (OS) at 2 years, with this being the most robust predictor as compared with the other analyzed parameters (figure 5C). In a multivariate model, we found that the CD103<sup>+</sup>CD49a<sup>+</sup>CD8<sup>+</sup> T-cell population remained predictive of survival when the model was adjusted for potential cofounders including PD-L1 expression and the infiltration of TCF1<sup>+</sup>CD8<sup>+</sup>T cells (table 1).

To confirm these results in a second cohort, we selected patients with NSCLC with PD-L1 expression on >50% of TCs who underwent first-line anti-PD-1 treatment (n=30) or second-line treatment (n=6). We found that only intratumoral infiltration by CD8<sup>+</sup> T<sub>RM</sub> cells co-expressing CD103 and CD49a was correlated with patient survival (HR=2.77 (1.13–6.75), p=0.025) (figure 6A), confirming the results obtained in the discovery cohort. Kaplan-Meier curves and log-rank tests (p=0.025) were used to analyze patients dichotomized based on median values (figure 6B). Tumor infiltration by the CD8<sup>+</sup> T<sub>RM</sub> cell population co-expressing CD103 and CD49a was also the only population correlated with PFS when using this same approach to patient dichotomization (HR=2.62 (1.18–5.81), p=0.018) (figure 6C).

## DISCUSSION

In this study, we have shown that the intratumoral CD8<sup>+</sup> T<sub>RM</sub> cell population co-expressing CD103 and CD49a was highly predictive of response to immunotherapy in two cohorts of patients with lung cancer undergoing first-line or second-line PD-1 blockade treatment. The predictive performance of this biomarker was also observed in a multivariate analysis. In contrast, the population of CD8<sup>+</sup>T<sub>RM</sub> cells expressing CD49a without CD103 was not associated with patient response to immunotherapy, irrespective of whether these cells were located in tumors or in the stroma. To the best of our knowledge, no study to date has analyzed the differential prognostic value of resident memory T-cell subpopulations. In most reports, CD103 expression alone has been used to define T<sub>RM</sub> populations. However, different T<sub>RM</sub> subpopulations have been defined according to a core marker profile that also includes CD49a and CD69.

Our CD103<sup>int</sup>CD49a<sup>+</sup>CD8<sup>+</sup> T<sub>RM</sub> population in mice displays other T<sub>RM</sub> characteristics such as CD69 expression and expresses transcription factors (Runx3, Hobit, Blimp1 and Notch1) associated with the T<sub>RM</sub> lineage, but not circulating markers such as SELL (online supplemental figure S4A). Previous results from our group and those of Topham showed that these populations persist in the lung in both cancer and infectious settings.<sup>10 33</sup>

Using single-cell analyses, other groups have identified T<sub>RM</sub> subpopulations in lung cancer at different stages of differentiation that share certain properties with our two populations, but their differential prognostic role has not been reported.<sup>15 34</sup> Previous work in melanoma

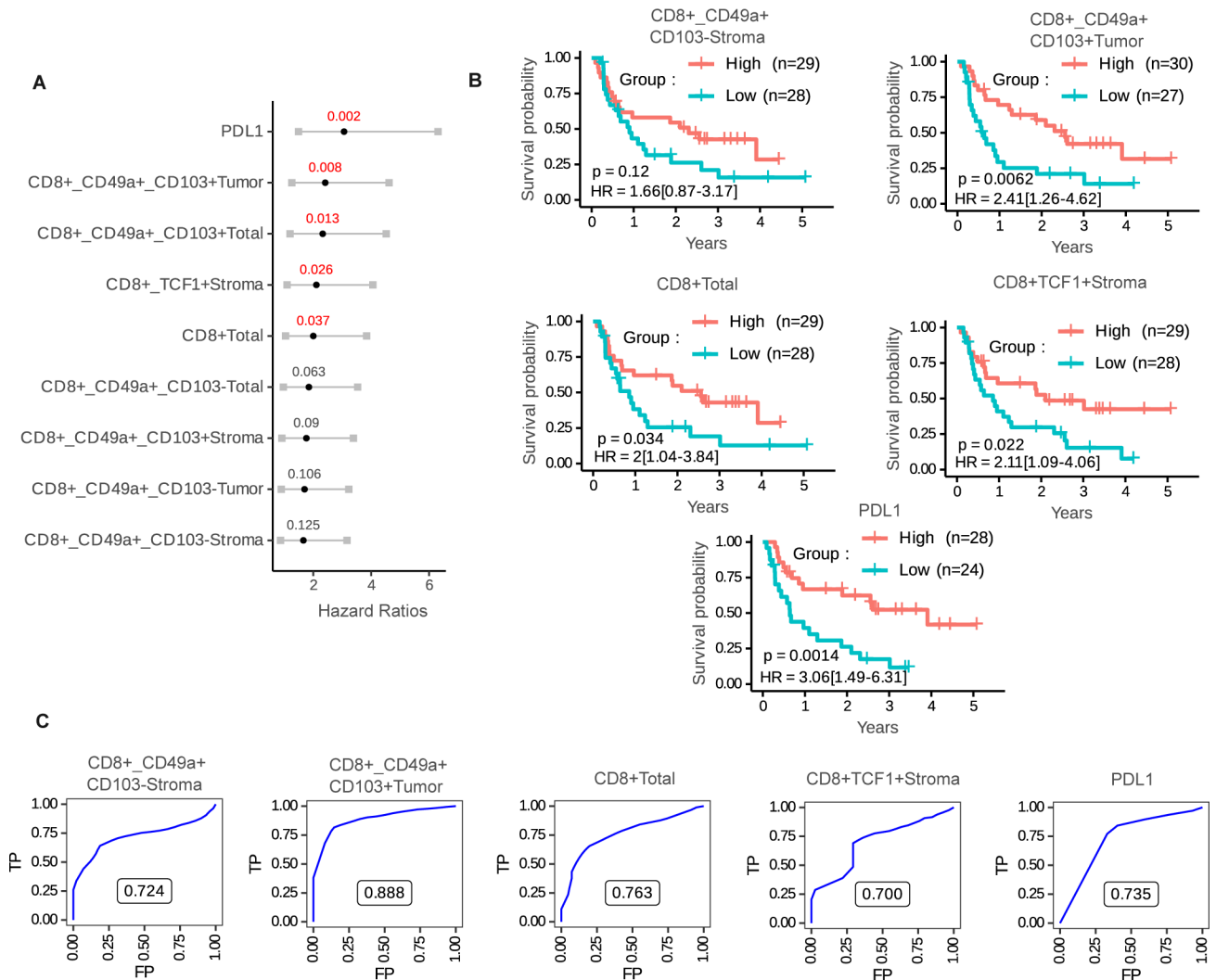


**Figure 5** Correlation between the infiltration of various subpopulations of CD8<sup>+</sup>T cells in the NSCLC tumor microenvironment on second line therapeutic and clinical outcomes. (A) Forest plot showing the HRs and 95% CIs computed using a univariate Cox model. The infiltration of several subsets of CD8<sup>+</sup>T cells and PD-L1 expression were quantified, using the median as a cut-off for dichotomization. Variables are ordered according to decreasing Wald statistic values. The sublocalization of these subpopulations in the stroma or the tumor or not (total) was taken into account. P value<0.05 was considered significant (in red). The HRs are calculated using the high group as a reference. A positive HR means that a high level of a measure is protective. (B) Kaplan-Meier curves corresponding to the overall survival of patients with NSCLC grouped according to tumorous or stromal infiltration by subpopulations of resident memory CD8<sup>+</sup>T cells or total TCF1<sup>+</sup>CD8<sup>+</sup>T cells and the expression of PD-L1 on tumor cells. Each variable was dichotomized separately based on the median value in order to define low and high groups. Log-rank test values are first displayed together with HRs, 95% CIs, and p values from the Wald test computed using a univariate Cox model. (C) Time-dependent receiver operating characteristic curves were used to analyze the true positive (TP) rate (sensitivity) and false positive (FP) rate (1-specificity) of the two subpopulations of resident memory CD8<sup>+</sup>T cells, total CD8<sup>+</sup>T cells, TCF1<sup>+</sup>CD8<sup>+</sup>T cells, and PD-L1 when predicting 2-year overall survival. For each variable, only patients whose variable values were located in the extreme tertiles of the corresponding distribution were included. The resulting area under the curve values are shown. NSCLC, non-small cell lung cancer.

had shown that a gene signature corresponding to the CD103<sup>+</sup>CD49<sup>+</sup>CD8<sup>+</sup>T<sub>RM</sub> cell population was correlated with better overall patient survival.<sup>14</sup> The more protective effects of intratumorally rather than stromally localized CD103<sup>+</sup> expressing T<sub>RM</sub> observed in this study has also been reported previously in patients with melanoma, NSCLC, and endometrial cancer.<sup>11 13 35</sup>

To explain the positive relationship between the CD103<sup>+</sup>CD49<sup>+</sup>CD8<sup>+</sup>T cell population and OS, several hypotheses can be put forward. We have shown in mouse

models that CD103<sup>+</sup>CD49<sup>+</sup>CD8<sup>+</sup>T cells are more functional than CD103<sup>-</sup>CD49<sup>+</sup>CD8<sup>+</sup>T cells, even though they express higher levels of inhibitory receptors such as PD-1 in both humans and mice. These results were confirmed in humans using single-cell transcriptomic analysis, where DP CD8<sup>+</sup>T cells expressed more IFN- $\gamma$ , IL-2, CCL3 and CXCL13 transcripts (online supplemental figure S4B,C).

Other work has also shown that the CD103<sup>+</sup>T<sub>RM</sub> population is superior to its CD103<sup>-</sup> counterparts in the production of IFN- $\gamma$  and TNF- $\alpha$ .<sup>36</sup> The CD103<sup>+</sup>CD49<sup>+</sup>CD8<sup>+</sup>T<sub>RM</sub>

**Table 1** Multivariable model adjusted for PD-L1 level and total stromal TCF-1<sup>+</sup>CD8<sup>+</sup> T cells

Variable	N	HR	95% CI	P value
TCF-1 <sup>+</sup> CD8 <sup>+</sup> stroma	52	0.98	(0.96, 1.00)	0.12
PD-L1	52	0.99	(0.98, 1.00)	0.08
CD49a <sup>+</sup> CD103 <sup>+</sup> CD8 <sup>+</sup> T cells (tumor)	52			
Low tertile	14			
High+inter tertile	38	0.39	(0.16, 0.92)	0.03

Using Cox proportional hazard model, the value of intratumoral CD49a<sup>+</sup>CD103<sup>+</sup>CD8<sup>+</sup>T cells (divided in tertile) in predicting overall survival was evaluated in a multivariate analysis adjusted for PD-L1 and total TCF-1<sup>+</sup>CD8<sup>+</sup>T cells as continuous variables.

population in the epidermis has also been reported as being the most cytotoxic population.<sup>24</sup>

It may seem paradoxical that the most exhausted population of T<sub>RM</sub> coexpressing CD103 and CD49a is the most functional and associated with a better prognosis. While some studies correlate exhaustion with poor clinical outcomes,<sup>28,37</sup> others have defined a subpopulation of CD103<sup>+</sup>CD8<sup>+</sup>T<sub>RM</sub> cells that appear exhausted, but are also characterized by a proliferative signature and clonal expansion, as well as superior functionality, and are associated with good patient outcomes.<sup>26,38,39</sup>

To explain these contradictory results, it is worth noting that there are different stages of exhaustion that are not equivalent in terms of functionality,<sup>40</sup> and some markers of exhaustion may also, in some situations, correspond to markers of activation.<sup>24</sup> Furthermore, based on previous reports, it is likely that the CD103<sup>+</sup>CD49a<sup>+</sup>CD8<sup>+</sup>T cell population is enriched with

tumor-specific T cells. In Corgnac *et al*, we have shown that this population exhibits enhanced proliferation and cytotoxicity towards autologous TCs and frequently displays oligoclonal expansion of particular TCR-β clonotypes.<sup>13</sup> We have also shown that this population expresses high levels of PD-1, which is a marker of tumor-reactive TILs in melanoma. Finally, this CD103<sup>+</sup>CD49a<sup>+</sup>CD8<sup>+</sup>T cell population expressed high levels of CD39 (figure 2). The CD103<sup>+</sup>CD39<sup>+</sup> T-cell population reportedly has a stronger reactivity against tumors relative to other CD8<sup>+</sup> T-cell subpopulations.<sup>41,42</sup> In contrast, the CD103<sup>-</sup>CD49a<sup>+</sup>CD8<sup>+</sup>T cell population may be part of TILs that are not engaged with antigen.<sup>43</sup> Finally, the absence of CD103 in this CD103<sup>-</sup>CD49a<sup>+</sup>CD8<sup>+</sup>T cell population may affect the persistence of this population in the tumor microenvironment and explain its less significant protective role.<sup>44</sup> In addition, antibody blockade of CD103 or CD103 genetic deficiency results

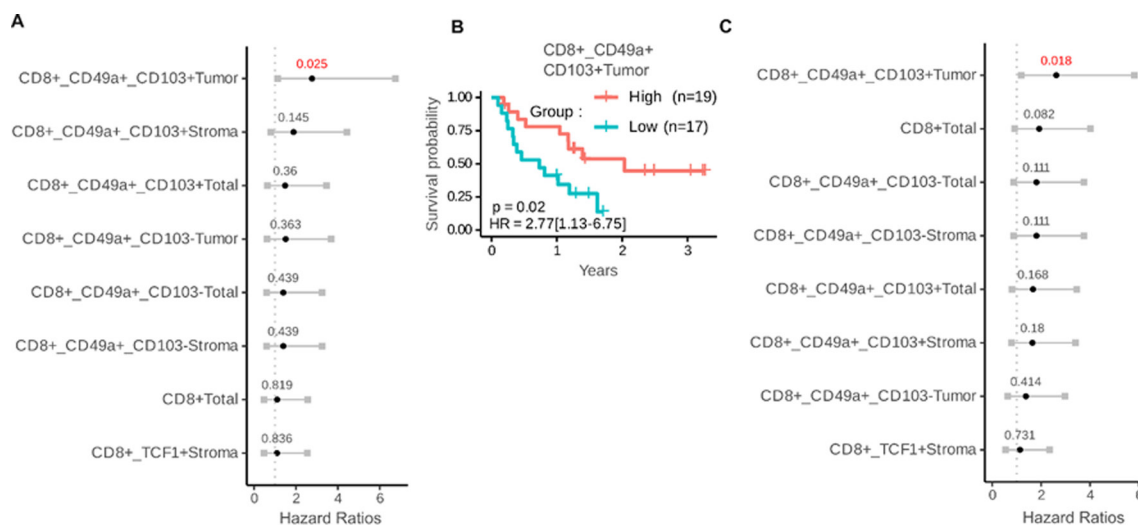


**Figure 6** The clinical impact of the infiltration of various subpopulations of CD8<sup>+</sup> T cells in the NSCLC tumor microenvironment in a validation cohort. (A) Forest plot representing Cox overall survival regression in patients with NSCLC (n=36). The infiltration of several subsets of CD8<sup>+</sup>T cells was quantified using the median as a cut-off. The sublocalization of these subpopulations in the stroma or the tumor or not (total) was taken into account. P value<0.05 was considered significant. (B) Kaplan-Meier analyses of the overall survival of patients with NSCLC depending on their level of intratumoral CD49a<sup>+</sup>CD103<sup>+</sup>CD8<sup>+</sup> T cells dichotomized with the median. Statistical analyses were performed with the log-rank test. (C) Forest plot representing Cox progression-free survival regression in patients with NSCLC (n=36). The infiltration of several subsets of CD8<sup>+</sup>T cells was quantified using the median as a cut-off. The sublocalization of these subpopulations in the stroma or the tumor or not (total) was taken into account. P value<0.05 was considered significant. The HRs are calculated using the high group as a reference. A positive HR means that a high level of a measure is protective. P value is indicated in red. NSCLC, non-small cell lung cancer.

in a reduction in tumor-infiltrating T cells and accelerated tumor progression in mice.<sup>45 46</sup>

Our work shows that there is a relationship between the two CD103<sup>+</sup>CD49a<sup>+</sup>CD8<sup>+</sup> and CD103<sup>+</sup>CD49a<sup>+</sup>CD8<sup>+</sup>T<sub>RM</sub> subpopulations, with the former appearing to be more differentiated than the latter. Indeed, these two populations share various TCRs that are amplified in the CD103<sup>+</sup>CD49a<sup>+</sup>CD8<sup>+</sup>T cell population. In addition, the CD103<sup>+</sup>CD49a<sup>+</sup>CD8<sup>+</sup>T cell population exhibits higher levels of TCF1 expression, a surrogate for progenitor cells, relative to the CD103<sup>+</sup>CD49a<sup>+</sup>CD8<sup>+</sup>T cell population. Other studies have reported common progenitor populations present in the blood that differentiate into distinct T<sub>RM</sub> subpopulations within tissues.<sup>38 44</sup> Furthermore, it has been shown that during T-cell priming, CD49a expression is induced in the lymph node, whereas CD103 expression is acquired after T-cell migration in the lung parenchyma and its expression kinetics are more delayed.<sup>45</sup> T<sub>RM</sub> differentiation in the lung parenchyma depends on the interaction of the T<sub>RM</sub> progenitor population with a specific DC population expressing CXCL16 and membrane IL-15.<sup>47</sup> Interestingly, the TCF1-expressing progenitor T-cell population has also been associated with response to immunotherapy in many cancers.<sup>28 30–32</sup> We also found that these stromal TCF1<sup>+</sup>CD8<sup>+</sup>T cells are able to predict responses to immunotherapy, although in a multivariate analysis, only the intratumoral CD103<sup>+</sup>CD49a<sup>+</sup>CD8<sup>+</sup>T<sub>RM</sub> population which does not express TCF1 remained statistically significant as a predictor of this clinical response.

With reference to previous studies showing that, in a tumor context, the classic T<sub>RM</sub> markers (CD103, CD69) do not clearly define their resident nature, we cannot guarantee that our T<sub>RM</sub> subpopulations defined by CD103 and CD49a markers are T<sub>RM</sub>.<sup>48</sup> Nevertheless, in Gavil's work, it was reported that tumor-specific resident CD8<sup>+</sup>TILs correlated best with markers of exhaustion (CD39, Tim-3), than with conventional resident markers. Our CD103<sup>+</sup>CD49a<sup>+</sup>CD8<sup>+</sup>T cell population expresses high levels of CD39 and Tim-3 compared with the CD103<sup>neg</sup>CD49a<sup>+</sup>CD8<sup>+</sup>T cell population. One hypothesis that is difficult to demonstrate in humans is that the CD103<sup>+</sup>CD49a<sup>+</sup>CD8<sup>+</sup>T cell population is more resident than the CD103<sup>neg</sup>CD49a<sup>+</sup>CD8<sup>+</sup>T cell population. However, in a previous work from our group, we showed that the longest-lasting predominant T<sub>RM</sub> population after vaccination was the CD103<sup>neg</sup>CD49a<sup>+</sup>CD8<sup>+</sup>T cell population.<sup>10</sup>

One of the limitations of this study analyzing and comparing the predictive value of subpopulations of T<sub>RM</sub> as a parameter of response to immunotherapy is that it was performed against total CD8, TCF1<sup>+</sup> progenitor T cells, and PD-L1, but not against markers of spatial interactions between PD-1 and PD-L1 or PD-L1 and CD8. These emerging biomarkers have also been reported to predict response to immunotherapy in NSCLC.<sup>49 50</sup>

This work provides a better understanding of why the CD103<sup>+</sup>CD49a<sup>+</sup>CD8<sup>+</sup>T<sub>RM</sub> population induced after systemic vaccination does not inhibit tumor growth, in contrast to the CD103<sup>+</sup>CD49a<sup>+</sup>T cell population induced

by i.n immunization.<sup>10</sup> We have previously shown that anti-CD49a antibodies reverse the therapeutic effect of the nasally administered vaccines, but were unable to distinguish which subpopulation (CD103<sup>+</sup> or CD103<sup>neg</sup>) of T<sub>RM</sub> expressing CD49a was targeted by the vaccine.<sup>9</sup> Cell transfer experiments were inconclusive.<sup>9 10</sup> This strengthens the rationale for mucosal vaccination to induce this protective T<sub>RM</sub> subpopulation coexpressing CD103 and CD49a.

In clinical practice, patients with lung cancer expressing >50% PD-L1 are treated with anti-PD-1 alone or in combination with chemotherapy. The quantification of the intratumoral T<sub>RM</sub> subpopulation co-expressing CD103 and CD49a could help guide clinical decision-making when considering these different therapeutic options.

## METHODS

Sex was not considered as a clinical variable in this study.

Investigators have been blinded to the patient clinical outcome during the experiment.

### Patient sample collection

Two tumor collections from patients with lung cancer were provided for this study: (1) A col checkpoint cohort which included tumor tissues from patients with lung cancer treated with anti-PD-1 (pembrolizumab or nivolumab) at the Hôpital Européen Georges Pompidou, regardless of the therapeutic line (first or second line or beyond). Pre-therapeutic biopsies (<6 months before the start of immunotherapy) were preferred for most patients, but archival biopsies were also available for some patients. This collection started in June 2016. The clinical database was available for this cohort through a local data warehouse (Bastien Rance); (2) The CERTIM (Immunomodulatory Therapies Multidisciplinary Study group) collection was created in February 2015 by Pr F Goldwasser (Department of Medical Oncology, Hôpital Cochin) and is a collaborative French multidisciplinary network of physicians involved in oncology and research, based at the Cochin Hospital (Paris, France). For this study, it enrolled patients with lung cancer treated with anti-PD-1 agents (nivolumab or pembrolizumab). At least one tumor biopsy was available for each patient included in the CERTIM cohort with a varying length of time before the start of immunotherapy, as well as a clinical database for each patient.

From these two collections, we selected a discovery cohort of 57 patients with lung cancer who underwent second line treatment with anti-PD-1 and a validation cohort of 36 patients, 30 of whom underwent first line anti-PD-1 treatment and 6 of whom underwent second line treatment, and for whom tumor tissue from lung localization was available to avoid bias due to localization to other sites.

Flow chart analyses for these cohorts are shown in online supplemental figure S1. Characteristics of these

two cohorts are presented in online supplemental tables S1 and S2.

### Experimental animals

Wild-type female C57BL/6J mice were purchased from Janvier Labs. Experiments were performed using mice 8–10 weeks of age. All mice were housed in an INSERM U970-PARCC animal facility under specific pathogen-free conditions. Experimental protocols were approved by ethical committee of Université Paris Cité (CEEA 34; approval MESR29315) in accordance with European guidelines (EC2010/63)

### Murine vaccination and sample preparation

STxB-E7 is a DC target-based vaccine chemically linked to the HPV16 E7<sub>43–57</sub> antigen as described previously.<sup>51</sup> Anesthetized mice were immunized twice on day 0 and day 14 via i.n or i.m. vaccination using STxB-E7, with  $\alpha$ -GalCer as an adjuvant (Funakoshi, Tebu-bio France). On day 21, mice were sacrificed. Intravascular staining was performed to discriminate between tissue-localized and blood-borne cells as described by Anderson *et al.*<sup>52</sup> Briefly, 5  $\mu$ g of anti-CD8 $\alpha$  APC-eFluo 780 (clone 53-6-7, eBioscience/Thermo Fisher) was injected intravenously 3 min prior to BAL and tissue collection. BAL was collected from anesthetized mice by flushing the lungs with phosphate-buffered saline (PBS)-EDTA (0.5 mM) via a cannula inserted into the trachea (5 washes  $\times$  1 mL).

Lungs were perfused with PBS-EDTA (0.5 mM) and digested in Roswell Park Memorial Institute Medium (RPMI)-1640 medium containing 1 mg/mL collagenase type IV (Life Technologies/Thermo Fisher) and 30  $\mu$ g/mL DNase I (Roche). Lung cells were dissociated using the gentleMACS (Miltenyi Biotec, France) lung programs 1 and 2, with gentle shaking for 30 min at 37°C between both steps. Then, the obtained single-cell suspensions were filtered through a 70  $\mu$ m strainer, washed with PB containing 2% fetal bovine serum (FBS), suspended in a 40% Percoll solution, layered over a 75% Percoll solution (Sigma-Aldrich), and centrifuged for 20 min at room temperature (RT) at 600 $\times$ g. Cells at the interface layer were collected and washed.

After FcR blocking with CD16/32 Ab (clone 93, eBioscience/Life Technologies), cells were first incubated for 30 min at RT with PE-conjugated H-2D<sup>b</sup>-E7<sub>49–57</sub> dextramers (Immudex, Bredevej 2A, 2830 Virum, Denmark). Then, cells were washed and stained for surface molecules for 20 min at 4°C in PBS-2%FBS containing anti-mouse CD8 $\beta$  BUV495 (clone YTS156, eBioscience), CD3 PerCP-Cy5.5 (clone 145-2C11, eBioscience/Life Technologies), CD103 Pacific Blue (clone 2E7, BioLegend), CD49a APC or vioFITC (Miltenyi Biotec), and CD69 (clone H1.2F3, BioLegend). For intracellular staining, after surface staining, cells were permeabilized using the FoxP3/transcription factor staining buffer set (eBiosciences) according to the manufacturer's protocols, after which they were stained with an intracellular monoclonal antibody (mAb) specific for Tcf1 (clone FAB8224R,

Bio-Techne). All the cells were labeled using the Live/Dead Cell Aqua Blue Viability Dye (Life Technologies). Data acquisition was performed with a BD Fortessa X-20 instrument (Becton Dickinson), and data from live single cells were analyzed using the FlowJo Software (Tree Star). Tissue-localized CD8<sup>+</sup>T cells were defined as CD3<sup>+</sup>CD8 $\alpha$ <sup>+</sup>CD8 $\beta$ <sup>+</sup> cells. The adjuvant C-Di-GMP was purchased from InvivoGen (Toulouse, France).

### Flow cytometry analyses of TILs

Freshly resected lung tumors and adjacent healthy lung tissue samples obtained from the Institut Mutualiste Montsouris and the Hôpital Marie-Lannelongue were immediately cut into small fragments and digested for 40 min at 37°C using a Tumor Dissociation Kit (Miltenyi Biotec). The dissociated samples were smashed on 100  $\mu$ m cell strainers, washed, and red blood cell lysis was performed. The recovered single-cell suspension was used for phenotypic analyses performed by direct immunofluorescence with a panel of fluorochrome-conjugated antibodies. Anti-CD3-Alexa 700 (UCHT1), anti-CD8-Pacific Blue (RPA-T8), anti-CD69-APC-Cy7 (FN50), anti-granzyme-B-FITC (GB11) were supplied by BioLegend. Anti-CD103-BV711 (Ber-ACT8) and anti-Hobit-Alexa 647 (Sanquin-Hobit/1) were purchased from BD Biosciences. Anti-CD49-PerCP-eFluo 710 (TS2/7) and anti-PD-1-PeCy7 (eBioJ105) were supplied by Thermo Fisher Scientific. Anti-RUNX3-PE (R3-5G4) and CCR7-PeCy7 (3D12) were purchased from BD Pharmingen. Anti-CD45RA-APC and anti-CD39-APC, were purchased from Miltenyi. Cells were fixed, permeabilized (FoxP3 Buffer Kit, eBioscience) and then stained with fluorochrome-conjugated mAbs. Dead cells were excluded using a LIVE/DEAD Fixable UV Dead Cell Stain Kit (Thermo Fisher Scientific). Stained cells were analyzed by flow cytometry using a BD FACS Fortessa flow cytometer (BD Biosciences). Data were processed using FlowJo Software (Tree Star).<sup>53</sup> This study was approved by the Institutional Review Board of Gustave Roussy (Commission scientifique des Essais thérapeutiques (CSET)) and informed consent was obtained.

### Multiplex immunofluorescence staining

T<sub>RM</sub> cell infiltration was assessed using formalin-fixed paraffin-embedded slides (4  $\mu$ m-thick sections) stained with a panel that had been developed manually before being automated with a Leica Bond robot (Leica Biosystems, Wetzlar, Germany). Slides were deparaffinized (Bond Dewax Solution, Leica Biosystems) and then rehydrated via immersion in decreasing concentrations of ethanol in distilled water. Slides were then fixed in 4% paraformaldehyde. Heating mediated-epitope/antigen retrieval was performed with Bond TM Epitope Retrieval 2 (Leica Biosystems). Blocking was performed with plant-based protein blocking buffer (Cell Signaling Technology (CST), Massachusetts, USA) for 15 min. Primary mAbs directed against selected antigens were diluted in SignalStain Antibody Diluent (CST) and incubated for 30 min (except for CD49a, 60 min). Secondary antibodies

conjugated to horseradish peroxidase (ImmunoReagents, North Carolina, USA) were then incubated on samples for 15 min (except for CD49a, 45 min). Finally, immunofluorescence labeling was performed with the CF Dye Tyramide from Biotium (California, USA). The slides were then washed and heated to remove non-adsorbed antibodies/dye, followed by saturation, labeling with the primary and secondary antibodies, repeating this as many times as necessary to achieve multiplexed labeling. The specificity of each antibody was validated using an isotype control.

The list of antibodies and reagents is provided in online supplemental table S3. After the final labeling, samples were stained with 4',6-diamidino-2-phenylindole (DAPI for nuclear counterstaining (PerkinElmer, Massachusetts, USA) and mounted in EverBrite Mounting Medium (Biotium).

### Multispectral imaging and phenotyping

Biopsies were whole-slide scanned using the Vectra System (PerkinElmer) at 20× magnification. 10 regions of interest were then selected using Phenochart whole-slide reviewer (PerkinElmer). A spectral library enabling the unmixing of dye was prepared using unstained and single-stained tonsil tissues. The inForm Cell Analysis software (PerkinElmer) was used to facilitate cell segmentation and phenotyping based in part on DAPI staining. A phenotyping step was then performed by training the software to recognize cells depending on their expressed surface biomarkers in order to define an analytical algorithm. Cells were then manually checked until the automatized recognition by inForm was consistent with the visual count. Each phenotype image was checked after software analysis. The inForm software provides a CI for each phenotyped cell. For the final statistical analysis, cells were taken into account only if the given CI was over 55% for the corresponding phenotype. The data was then analyzed using R software and the phenoptrReports package (Akoya).

The segmentation between stroma and tumor area was achieved by staining for E-cadherin, which labels TCs.

### In vitro stimulation and multiplex cytokine assay

Single-cell preparations were obtained from the BAL and lungs of mice on day 21 after i.n vaccination as described previously. Total CD8<sup>+</sup> T cells were isolated by magnetic sorting (EasySep Mouse CD8<sup>+</sup> T Cell Isolation Kit, STEMCELL Technologies), followed by tetramer E7 and T<sub>RM</sub> marker staining. Then, E7-specific T<sub>RM</sub> CD103<sup>+</sup>CD49a<sup>+</sup>, CD103<sup>neg</sup>CD49a<sup>+</sup>, and Teff CD103<sup>neg</sup>CD49a<sup>neg</sup> populations were sorted by flow cytometry and stimulated (10,000 cells/well) with E7<sub>49-57</sub> peptide (10 µg/mL) for 18 hours. Then, supernatants were harvested and a bead-based multiplexed cytokine immunoassay was performed to detect IL-2, IFN-γ, granzyme B, MIP1a/CCL3, MIP1b/CCL4, and RANTES/CCL5 (R&D Bio-Techne) according to the manufacturer's protocol and analyzed using the Bio-Plex 200 platform (Bio-Rad). Analyte concentrations were calculated using a standard curve (5 PL regression) with the Bio-Plex manager software.

### Statistical analysis

All statistical analyses were performed using R V.3.4.2. Kaplan-Meier curves (to visualize survival probabilities) and log-rank tests (to test for statistical significance between groups) were performed using the ggsurvplot function of the survminer package. Univariate analyses for both OS and PFS were conducted using a Cox proportional hazards model implemented in the coxph function of the survival package, retrieving HRs, 95% CIs, and Wald statistics to address the statistical significance of the model. For each variable of interest, the data were dichotomized into "Low" and "High" groups according to the median or extreme tertile cut-offs of the distribution for the univariate survival analysis.

Time-dependent ROC curve and AUC (area under the curve) analyses were conducted with the survival ROC package configured using the nearest neighbor estimation method. The Cox proportional hazard model was also used to perform a multivariate analysis to assess whether the prognostic effect of a variable of interest remains significant after adjustment for other potential cofounders. These variables were considered as continuous variables whereas the variable of interest was dichotomized into two groups.

Details on PD-L1 expression, single cell and TCR analysis are provided as supplementary data.

### Author affiliations

<sup>1</sup>Université Paris Cité, INSERM, PARCC, Paris, France, Paris, France

<sup>2</sup>INSERM UMR1186, Gustave Roussy, Fac.de Medecine-Univ Paris-Sud, Université Paris-Saclay, Villejuif, France, INSERM, Villejuif, France

<sup>3</sup>INSERM U1194, Institut de Recherche en Cancérologie de Montpellier, Montpellier, France

<sup>4</sup>Service de Pneumologie Hopital Cochin, Université de Paris, Paris, France

<sup>5</sup>Centre de recherche des Cordeliers, Université Paris Cité, Sorbonne Université, INSERM UMRS1138, Paris, France

<sup>6</sup>Department of Medical Oncology, Université Paris Cité, Cochin Hospital, APHP, Paris, France

<sup>7</sup>Cellular and Chemical Biology Unit, Institut Curie, Paris, France

<sup>8</sup>Department Immunology, Hôpital Européen Georges Pompidou, Hopital Necker, APHP, Paris, France

<sup>9</sup>Parean Biotech, Saint Malo, France

<sup>10</sup>Diversity and plasticity of childhood tumours lab, INSERM U830 Equipe Labellisée Ligue Nationale contre le Cancer, PSL Research University, Institut Curie Research Center, Paris, France

<sup>11</sup>Department of translational research, PSL Research University, Institut Curie Research Center, Paris, France

<sup>12</sup>Cytometry and Biomarkers UTEchs, Center for translational Science, Institut Pasteur, Paris, France

<sup>13</sup>Biochimie, Hôpital Européen Georges Pompidou, Paris, France

<sup>14</sup>Paris Cancer Institute Carpem, Paris, France

<sup>15</sup>Department Pathology, Hôpital Européen Georges Pompidou, Paris, France

<sup>16</sup>Onco-pneumology, Hopital Européen Georges Pompidou, Paris, France

<sup>17</sup>Departments of Pathology Hospital Cochin Assistance Publique Hopitaux de Paris, APHP, Paris, France

<sup>18</sup>Department of Pathology, Hopital Cochin, APHP, Paris, France

**Present affiliations** The present affiliation of Léa Paolini is Inserm UMR-1125, Bobigny, France and Sorbonne Paris Nord University, Bobigny, France.

**X** Isabelle Cremer @CremerIsabelle

**Acknowledgements** We thank the staff of the tumor banks of HEGP (B Védie and D Geromin) for providing the sample materials and the Histology platform of PARCC (C Lesaffre).

**Contributors** The guarantor of the study in the contributorship statement is ET. LP, TT and SC contributed to the conception of the work, acquisition, analysis,

interpretation of the data, and drafting of the manuscript. ET carried out the coordination of the work. DD contributed to the conception of the work, analyzed and interpreted the data and drafted the manuscript. J-PV, MW and JA contributed to the analysis, and interpretation of the data, as well as critically reviewing the manuscript. JP, AG, VQ, PB, MH, VL, SM and AC conducted experiments and contributed to analysis and interpretation of the data and review it critically. LJ, JU, L-VV, NG, SDP, PB-R, FG, IC, KL, PL-P, HDSB, LG, PR, FM-C and EF contributed to analysis and interpretation of the data and review it critically. All authors participated in final approval of the version to be published. LP, TT and SC participate in the conception of the work, they conduct experiments and acquired, analyzed and interpret the data as well as participation in the first drafting of the work. LP is first as she provided the figures 4 and 5 which could be considered slightly more important for the conclusion of the study.

**Funding** This work was funded by the Fondation ARC pour la Recherche sur le Cancer (Grant number SIGN'IT20181007747 and PGA 2020 12019110000946\_1581 to ET), the INCA (Institut National du Cancer) (Grant number 2022 PLBIO22-147 to ET), PCSI 2021 (M2DIA), the Agence Nationale de la Recherche (Labex Immuno-Oncology to ET), the Institut National du Cancer (Grant SIRIC CARPEM to ET and LP), FONCER (to ET), Fondation pour la Recherche Médicale (FRM) (EQU202103012926 to LJ), Institut National du Cancer (INCa) (contract n°2019-1-PLBIO-05-1 to ET and LJ), La Ligue contre le Cancer MucorNAVax (Convention N°AAPARN 2021. LCC/ChP to ET and LJ), PEPR RNAVax (ANR-22-PEBI-0007 to ET and LJ).

**Competing interests** None declared.

**Patient consent for publication** Not applicable.

**Ethics approval** This study involves human participants and was approved by CPP Ile de France II (CPP number : 2015-08-04-MS2) and the CNIL declaration (IDP1563364). Participants gave informed consent to participate in the study before taking part.

**Provenance and peer review** Not commissioned; externally peer reviewed.

**Data availability statement** Data are available upon reasonable request. Single-cell RNA sequencing data were uploaded to the NCBI Gene Expression Omnibus (GEO) archive platform (<https://www.ncbi.nlm.nih.gov/geo/>) under accession number GSE280433.

**Supplemental material** This content has been supplied by the author(s). It has not been vetted by BMJ Publishing Group Limited (BMJ) and may not have been peer-reviewed. Any opinions or recommendations discussed are solely those of the author(s) and are not endorsed by BMJ. BMJ disclaims all liability and responsibility arising from any reliance placed on the content. Where the content includes any translated material, BMJ does not warrant the accuracy and reliability of the translations (including but not limited to local regulations, clinical guidelines, terminology, drug names and drug dosages), and is not responsible for any error and/or omissions arising from translation and adaptation or otherwise.

**Open access** This is an open access article distributed in accordance with the Creative Commons Attribution Non Commercial (CC BY-NC 4.0) license, which permits others to distribute, remix, adapt, build upon this work non-commercially, and license their derivative works on different terms, provided the original work is properly cited, appropriate credit is given, any changes made indicated, and the use is non-commercial. See <http://creativecommons.org/licenses/by-nc/4.0/>.

#### ORCID iDs

Marie Wislez <http://orcid.org/0000-0001-7518-7859>

Nadège Gruel <http://orcid.org/0000-0001-6915-8082>

Isabelle Cremer <http://orcid.org/0000-0002-0963-1031>

Karen Leroy <http://orcid.org/0000-0002-4379-0140>

Eric Tartour <http://orcid.org/0000-0002-7323-468X>

#### REFERENCES

- Masopust D, Vezyz V, Marzo AL, *et al.* Preferential Localization of Effector Memory Cells in Nonlymphoid Tissue. *Science* 2001;291:2413–7.
- Hombrink P, Helbig C, Backer RA, *et al.* Programs for the persistence, vigilance and control of human CD8+ lung-resident memory T cells. *Nat Immunol* 2016;17:1467–78.
- Kumar BV, Ma W, Miron M, *et al.* Human Tissue-Resident Memory T Cells Are Defined by Core Transcriptional and Functional Signatures in Lymphoid and Mucosal Sites. *Cell Rep* 2017;20:2921–34.
- Mami-Chouaib F, Blanc C, Corgnac S, *et al.* Resident memory T cells, critical components in tumor immunology. *J Immunother Cancer* 2018;6:87.
- Schenkel JM, Masopust D. Tissue-Resident Memory T Cells. *Immunity* 2014;41:886–97.
- Ariotti S, Hogenbirk MA, Dijkgraaf FE, *et al.* T cell memory. Skin-resident memory CD8(+) T cells trigger a state of tissue-wide pathogen alert. *Science* 2014;346:101–5.
- Ge C, Monk IR, Pizzolla A. Bystander Activation of Pulmonary Trm Cells Attenuates the Severity of Bacterial Pneumonia by Enhancing Neutrophil Recruitment. *Cell Rep* 2019;29:4236–44.
- Iijima N, Iwasaki A. T cell memory. A local macrophage chemokine network sustains protective tissue-resident memory CD4 T cells. *Science* 2014;346:93–8.
- Sandoval F, Terme M, Nizard M, *et al.* Mucosal imprinting of vaccine-induced CD8+ T cells is crucial to inhibit the growth of mucosal tumors. *Sci Transl Med* 2013;5:172ra20.
- Nizard M, Roussel H, Diniz MO, *et al.* Induction of resident memory T cells enhances the efficacy of cancer vaccine. *Nat Commun* 2017;8:15221.
- Djenidi F, Adam J, Goubar A, *et al.* CD8+CD103+ tumor-infiltrating lymphocytes are tumor-specific tissue-resident memory T cells and a prognostic factor for survival in lung cancer patients. *J Immunol* 2015;194:3475–86.
- Ganesan AP, Clarke J, Wood O, *et al.* Tissue-resident memory features are linked to the magnitude of cytotoxic T cell responses in human lung cancer. *Nat Immunol* 2017;18:940–50.
- Corgnac S, Malenica I, Mezquita L, *et al.* CD103(+)CD8(+) TRM Cells Accumulate in Tumors of Anti-PD-1-Responder Lung Cancer Patients and Are Tumor-Reactive Lymphocytes Enriched with Tc17. *Cell Rep Med* 2020;1:100127.
- Zitti B, Hoffer E, Zheng W, *et al.* Human skin-resident CD8+ T cells require RUNX2 and RUNX3 for induction of cytotoxicity and expression of the integrin CD49a. *Immunity* 2023;56:1285–302.
- Banchereau R, Chitre AS, Scherl A, *et al.* Intratumoral CD103+ CD8+ T cells predict response to PD-L1 blockade. *J Immunother Cancer* 2021;9:e002231.
- Attrill GH, Owen CN, Ahmed T, *et al.* Higher proportions of CD39+ tumor-resident cytotoxic T cells predict recurrence-free survival in patients with stage III melanoma treated with adjuvant immunotherapy. *J Immunother Cancer* 2022;10:e004771.
- Luoma AM, Suo S, Wang Y, *et al.* Tissue-resident memory and circulating T cells are early responders to pre-surgical cancer immunotherapy. *Cell* 2022;185:2918–35.
- Edwards J, Wilmott JS, Madore J, *et al.* CD103+ Tumor-Resident CD8+ T Cells Are Associated with Improved Survival in Immunotherapy-Naïve Melanoma Patients and Expand Significantly During Anti-PD-1 Treatment. *Clin Cancer Res* 2018;24:3036–45.
- Virassamy B, Caramia F, Savas P, *et al.* Intratumoral CD8+ T cells with a tissue-resident memory phenotype mediate local immunity and immune checkpoint responses in breast cancer. *Cancer Cell* 2023;41:585–601.
- Yost KE, Satpathy AT, Wells DK, *et al.* Clonal replacement of tumor-specific T cells following PD-1 blockade. *Nat Med* 2019;25:1251–9.
- Jeyanathan M, Fritz DK, Afkhami S, *et al.* Aerosol delivery, but not intramuscular injection, of adenovirus-vectored tuberculosis vaccine induces respiratory-mucosal immunity in humans. *JCI Insight* 2022;7.
- Douguet L, Fert I, Lopez J, *et al.* Full eradication of pre-clinical human papilloma virus-induced tumors by a lentiviral vaccine. *EMBO Mol Med* 2023;15:e17723.
- Künzli M, O'Flanagan SD, LaRue M, *et al.* Route of self-amplifying mRNA vaccination modulates the establishment of pulmonary resident memory CD8 and CD4 T cells. *Sci Immunol* 2022;7:eadd3075.
- Cheuk S, Schlums H, Gallais Sérézal I, *et al.* CD49a Expression Defines Tissue-Resident CD8 + T Cells Poised for Cytotoxic Function in Human Skin. *Immunity* 2017;46:287–300.
- Bergsbaken T, Bevan MJ. T cells responding to infection. *Nat Immunol* 2015;16:406–14.
- Clarke J, Panwar B, Madrigal A, *et al.* Single-cell transcriptomic analysis of tissue-resident memory T cells in human lung cancer. *J Exp Med* 2019;216:2128–49.
- Wu J, Madi A, Mieg A, *et al.* T Cell Factor 1 Suppresses CD103+ Lung Tissue-Resident Memory T Cell Development. *Cell Rep* 2020;31:107484.
- Sade-Feldman M, Yizhak K, Bjorgaard SL, *et al.* Defining T Cell States Associated with Response to Checkpoint Immunotherapy in Melanoma. *Cell* 2018;175:998–1013.
- Aman J, Margadant C. Integrin-Dependent Cell-Matrix Adhesion in Endothelial Health and Disease. *Circ Res* 2023;132:355–78.

- 30 Kurtulus S, Madi A, Escobar G, *et al.* Checkpoint Blockade Immunotherapy Induces Dynamic Changes in PD-1–CD8+ Tumor-Infiltrating T Cells. *Immunity* 2019;50:181–94.
- 31 Miller BC, Sen DR, Al Abosy R, *et al.* Subsets of exhausted CD8+ T cells differentially mediate tumor control and respond to checkpoint blockade. *Nat Immunol* 2019;20:326–36.
- 32 Siddiqui I, Schaeuble K, Chennupati V. Intratumoral Tcf1+PD-1+CD8+ T Cells with Stem-like Properties Promote Tumor Control in Response to Vaccination and Checkpoint Blockade Immunotherapy. *Immunity* 2019;50:195–211.
- 33 Reilly EC, Sportiello M, Emo KL, *et al.* CD49a Identifies Polyfunctional Memory CD8 T Cell Subsets that Persist in the Lungs After Influenza Infection. *Front Immunol* 2021;12:728669.
- 34 Guo X, Zhang Y, Zheng L, *et al.* Global characterization of T cells in non-small-cell lung cancer by single-cell sequencing. *Nat Med* 2018;24:978–85.
- 35 Workei HH, Komdeur FL, Wouters MCA, *et al.* CD103 defines intraepithelial CD8+ PD1+ tumour-infiltrating lymphocytes of prognostic significance in endometrial adenocarcinoma. *Eur J Cancer* 2016;60:1–11.
- 36 Watanabe R, Gehad A, Yang C, *et al.* Human skin is protected by four functionally and phenotypically discrete populations of resident and recirculating memory T cells. *Sci Transl Med* 2015;7:279ra39.
- 37 Datar I, Sanmamed MF, Wang J, *et al.* Expression Analysis and Significance of PD-1, LAG-3, and TIM-3 in Human Non-Small Cell Lung Cancer Using Spatially Resolved and Multiparametric Single-Cell Analysis. *Clin Cancer Res* 2019;25:4663–73.
- 38 Gueguen P, Metoikidou C, Dupic T, *et al.* Contribution of resident and circulating precursors to tumor-infiltrating CD8+ T cell populations in lung cancer. *Sci Immunol* 2021;6:eabd5778.
- 39 Thommen DS, Koelzer VH, Herzig P, *et al.* A transcriptionally and functionally distinct PD-1+ CD8+ T cell pool with predictive potential in non-small-cell lung cancer treated with PD-1 blockade. *Nat Med* 2018;24:994–1004.
- 40 Giles JR, Globig A-M, Kaech SM, *et al.* CD8+ T cells in the cancer-immunity cycle. *Immunity* 2023;56:2231–53.
- 41 Simoni Y, Becht E, Fehlings M, *et al.* Bystander CD8+ T cells are abundant and phenotypically distinct in human tumour infiltrates. *Nature New Biol* 2018;557:575–9.
- 42 Chow A, Uddin FZ, Liu M, *et al.* The ectonucleotidase CD39 identifies tumor-reactive CD8+ T cells predictive of immune checkpoint blockade efficacy in human lung cancer. *Immunity* 2023;56:93–106.
- 43 Melssen MM, Lindsay RS, Stasiak K, *et al.* Differential Expression of CD49a and CD49b Determines Localization and Function of Tumor-Infiltrating CD8+ T Cells. *Cancer Immunol Res* 2021;9:583–97.
- 44 Mackay LK, Rahimpour A, Ma JZ, *et al.* The developmental pathway for CD103+CD8+ tissue-resident memory T cells of skin. *Nat Immunol* 2013;14:1294–301.
- 45 Murray T, Fuertes Marraco SA, Baumgaertner P, *et al.* Very Late Antigen-1 Marks Functional Tumor-Resident CD8 T Cells and Correlates with Survival of Melanoma Patients. *Front Immunol* 2016;7:573.
- 46 Malik BT, Byrne KT, Vella JL, *et al.* Resident memory T cells in the skin mediate durable immunity to melanoma. *Sci Immunol* 2017;2:eaam6346.
- 47 Di Pilato M, Kfuri-Rubens R, Pruessmann JN, *et al.* CXCR6 positions cytotoxic T cells to receive critical survival signals in the tumor microenvironment. *Cell* 2021;184:4512–30.
- 48 Gavil NV, Scott MC, Weyu E, *et al.* Chronic antigen in solid tumors drives a distinct program of T cell residence. *Sci Immunol* 2023;8:eadd5976.
- 49 Sánchez-Magraner L, Gumuzio J, Miles J, *et al.* Functional Engagement of the PD-1/PD-L1 Complex But Not PD-L1 Expression Is Highly Predictive of Patient Response to Immunotherapy in Non-Small-Cell Lung Cancer. *J Clin Oncol* 2023;41:2561–70.
- 50 Ghiringhelli F, Bibeau F, Greillier L, *et al.* Immunoscore immune checkpoint using spatial quantitative analysis of CD8 and PD-L1 markers is predictive of the efficacy of anti-PD1/PD-L1 immunotherapy in non-small cell lung cancer. *EBioMedicine* 2023;92:104633.
- 51 Karaki S, Blanc C, Tran T, *et al.* CXCR6 deficiency impairs cancer vaccine efficacy and CD8+ resident memory T-cell recruitment in head and neck and lung tumors. *J Immunother Cancer* 2021;9:e001948.
- 52 Anderson KG, Sung H, Skon CN, *et al.* Cutting Edge: Intravascular Staining Redefines Lung CD8 T Cell Responses. *J Immunol* 2012;189:2702–6.
- 53 Corgnac S, Lecluse Y, Mami-chouaib F. Isolation of tumor-resident CD8+ T cells from human lung tumors. *STAR Protocols* 2021;2:100267.